

Terahertz time-domain spectroscopy to probe laser-excited spin currents in a Co/Gd system

Fan Zhang(张帆), Bin Hong(洪宾), Michel Hehn, Rongqing Zhao(赵戎庆), Gregory Malinowski, Yong Xu(许涌), Stéphane Mangin, Jon Gorchon, and Weisheng Zhao(赵巍胜)

Citation: Chin. Phys. B, 2025, 34 (**12**): 126701. DOI: 10.1088/1674-1056/ade8e7
http://cpb.iphy.ac.cn; http://iopscience.iop.org/cpb

What follows is a list of articles you may be interested in

Exciton and valley dynamics in WSe_2/GaAs heterostructure

Xin Wei(魏鑫), Yuanhe Li(李元和), Wenkai Zhu(朱文凯), Rongkun Han(韩荣坤), Jianhua Zhao(赵建华), Kaiyou Wang(王开友), and Xinhui Zhang(张新惠)
Chin. Phys. B, 2025, 34 (**9**): 096701. DOI: 10.1088/1674-1056/add504

Spin detection and manipulation with scanning tunneling microscopy

Chunlei Gao(高春雷)
Chin. Phys. B, 2018, 27 (**10**): 106701. DOI: 10.1088/1674-1056/27/10/106701

Liquid phase epitaxy magnetic garnet films and their applications

Yi-Heng Rao(饶毅恒), Huai-Wu Zhang(张怀武), Qing-Hui Yang(杨青慧), Dai-Nan Zhang(张岱南), Li-Chuan Jin(金立川), Bo Ma(马博), Yu-Juan Wu(吴玉娟)
Chin. Phys. B, 2018, 27 (**8**): 086701. DOI: 10.1088/1674-1056/27/8/086701

Spin-dependent balance equations in spintronics

Zheng-Chuan Wang(王正川)
Chin. Phys. B, 2018, 27 (**1**): 016701. DOI: 10.1088/1674-1056/27/1/016701

Terahertz time-domain spectroscopy to probe laser-excited spin currents in a Co/Gd system

Fan Zhang(张帆)[1], Bin Hong(洪宾)[2], Michel Hehn[3], Rongqing Zhao(赵戎庆)[1,4], Gregory Malinowski[3], Yong Xu(许涌)[4,†], Stéphane Mangin[3], Jon Gorchon[3,‡], and Weisheng Zhao(赵巍胜)[1,4]

[1] *Hefei Innovation Research Institute, Beihang University, Hefei* 230013, *China*
[2] *Center of Free Electron Laser & High Magnetic Field, Institute of Physical Science and Information Technology, Anhui University, Hefei* 230601, *China*
[3] *Université de Lorraine, CNRS, IJL, F-*54000 *Nancy, France*
[4] *Fert Beijing Institute, School of Integrated Circuit Science and Engineering, Beihang University, Beijing* 100191, *China*

(Received 2 May 2025; revised manuscript received 14 June 2025; accepted manuscript online 27 June 2025)

Single shot all-optical switching of the magnetization by femtosecond laser pulses in rare-earth transition-metal ferrimagnetic materials is particularly promising for future ultrafast magnetic storage applications. Moreover, ultrafast laser-generated spin currents appear to play an important role in the switching process. Here, we try to separately detect the spin current from Gd in a Co/Gd bilayer system using terahertz time-domain spectroscopy. To this aim, we use different capping, buffer and embedded layers in order to tune the spin-to-charge and spin-current propagation and identify currents from each of the layers. We attribute the observed THz emission in all layers to the transition metal demagnetization induced spin currents, and detect no contribution from the Gd demagnetization. We attribute this absence of Gd-induced THz signal to the potentially slow demagnetization of Gd, which shift the emission spectra to lower frequencies, below our detection capabilities. These results highlight the limitations in using materials suffering from the so-called critical slowdown for the optimization of spintronic THz emitters.

Keywords: Co/Gd bilayer, spin current, THz emission, demagnetization

PACS: 67.30.hj, 85.75.–d, 75.78.Jp

DOI: 10.1088/1674-1056/ade8e7 **CSTR:** 32038.14.CPB.ade8e7

1. Introduction

The development of ultrashort pulse lasers enables the study of ultrafast magnetization dynamics. Following the discovery of ultrafast demagnetization,[1] all-optical switching (AOS) of the magnetization of rare-earth transition-metal ferrimagnetic materials was demonstrated using femtosecond laser pulses,[2–4] which is particularly promising for potential future ultrafast information technologies.

In light of the technological potential of ultrafast magnetization dynamics, the underlying physics has attracted considerable interest.[5–11] Malinowski *et al.*[5] first demonstrated that laser-excited spin current transport could enhance and accelerate demagnetization in ferromagnetic multilayers due to the transfer of spin-angular-momentum between two thin ferromagnetic layers. Soon afterwards, Battiato *et al.*[6] proposed superdiffusive spin transport theory to explain laser-driven demagnetization. They suggested that the laser-excited spin majority carriers are much more mobile than spin minority carriers due to spin-dependent lifetimes and velocities, causing a net spin current to flow out of the ferromagnetic layer, leading to demagnetization. The laser-excited spin current has extended our understanding of the fundamental mechanisms behind ultrafast magnetization dynamics and has therefore attracted widespread attention. Recent studies have shown that the laser-excited spin current from the ferromagnet can influence the AOS process, and the magnetization of a ferromagnetic thin film can be reversed via spin current coming from the nearby switchable layer.[9,12–14] Thus, the spin current plays a critical role in the switching mechanism.

It is also worth noting that the timescales of laser-generated spin currents are on the subpicosecond timescale, corresponding to frequencies in the terahertz (THz) range. The spin currents can generate THz radiation through spin-to-charge conversion in strongly spin–orbit coupled materials. In recent years, a few THz studies have been carried out on Gd(Fe)Co and Co/Gd systems.[15–17] Using THz emission spectroscopy, Huisman *et al.*[15] found that under pulsed laser excitation, a spin current is generated from GdFeCo to the adjacent Pt layer even when the net magnetization is zero, due to the fact that the spin current is determined by the magnetic sublattice sensitivity. However, the contribution of each element to the spin current is not well understood so far.

In this work, we used a series of Co/Gd bilayer films to elucidate the contribution of Gd to ultrafast spin currents by

†Corresponding author. E-mail: yongxu@buaa.edu.cn
‡Corresponding author. E-mail: jon.gorchon@univ-lorraine.fr

© 2025 Chinese Physical Society and IOP Publishing Ltd. All rights, including for text and data mining, AI training, and similar technologies, are reserved.

using THz emission spectroscopy. We designed the sample structures by inserting MgO layer to block the transport of the spin current[18] and by changing the buffer and capping layers to change the spin-to-charge conversion, and collected their THz spectra. After analysis, we conclude that most of the THz emission is due to the transition metal-induced spin currents, and that detection of the Gd-induced THz is not possible using our setup.

2. Materials and methods

2.1. Samples fabrication and characterization

The Co/Gd samples that we used in our experiments were deposited by magnetron sputtering on a glass substrate (1-mm thick) in an argon atmosphere at a pressure of 3 mTorr (1 Torr $= 1.33322\times10^2$ Pa) and room temperature. The full sample stack is made of glass (substrate)/Ta(3)/Co(2)/Ta(5) or glass (substrate)/Ta(3)/Co(2)/Gd(1)/Ta(5) to first test THz emission from Gd. To test combinations of THz signal emissions, the structure glass (substrate)/*X*/Cu(4)/Co(2)/Gd(1)/Cu(4)/*Y* was used, where *X* and *Y* are buffer and capping layers of Ta(5) or Pt(3). Thin Cu layers were used to keep the interfaces with the magnetic layers constant. The Ta cap layer is slightly thicker than the buffer Ta or Pt cap as some surface oxidation is expected (a few nm). The numbers in brackets indicate the thickness in units of nm. In addition, some samples-included MgO layers introduced in the center of the Cu layers to block the ultrafast transport of laser-excited spin-polarized electrons.

To measure the THz emission spectra generated by Co/Gd samples upon femtosecond laser pulse excitation, we used a homemade THz time-domain spectrometer. The femtosecond laser pulses were generated by a commercial Ti:sapphire regenerative amplifier with a central wavelength of 800 nm, a pulse duration of 35 fs, and a repetition rate of 1 kHz. The pump beam with an incident power of 300 mW and a spot size of 10 mm (0.38 mJ/cm^2) was illuminated vertically on the sample. The residual pump beam after the sample was blocked by a piece of high-density polyethylene, which is transparent in the THz frequency range. The radiated THz pulses were detected with a 2-mm-thick ZnTe crystal via electro-optical sampling. The effective detection range of this THz time-domain spectrometer is mainly determined by the electro-optic crystal (0.1 THz–3 THz). During the experiment, an external in-plane magnetic field of 800 Oe is applied to orient the Co magnetization. All the experiments were performed at room temperature. When the pump beam impinged on the samples from the top (substrate) side, it is referred to as sample-t (-s) excitation (Fig. 1(a)). We added a bare glass substrate to the top of the film to minimize the effect of the substrate on the THz signal when flipping the sample.

3. Results and discussion

We first investigate by exploring simple, rather symmetric films, in order to compare the spin emission towards the top and bottom of the film. Figure 1(b) shows the THz waveforms generated from samples sub/Ta(3)/Co(2)/Ta(5) and sub/Ta(3)/Co(2)/Gd(1)/Ta(5). It can be seen that the sign of the emitted THz radiation reverses when the sample is rotated 180° around the vertical axis. The sub/Ta/Co/Ta sample emits THz radiation via the inverse spin Hall effect (ISHE) in both Ta layers. The generated charge current can be described with $\boldsymbol{j}_c \propto \boldsymbol{j}_s \times \boldsymbol{M}/|\boldsymbol{M}|$, where $\boldsymbol{j}_c$ is the charge current, $\boldsymbol{j}_s$ is the spin current, and $\boldsymbol{M}$ is the magnetization.[19] In our experiment, the external magnetic field direction was fixed, so the sign of the generated THz waveforms should depend on the sample orientation relative to the pump beam, which is consistent with the experimental results. In the Ta/Co/Ta film, the spin currents into both top and bottom Ta layers will lead to THz waves with opposite phase, which will destructively interfere (Fig. 1(c)), but due to small asymmetries, a net THz amplitude can still be measured (Fig. 1(b)). The insertion of the Gd layer causes the THz signal to increase in amplitude without changing sign, as shown in orange in Fig. 1(b). In the sub/Ta/Co/Gd/Ta sample, the magnetization of Gd and Co is antiparallelly aligned.[20] Although bulk Gd is paramagnetic at room temperature, it can stabilize a ferromagnetic phase when interfaced with a ferromagnetic material.[21] If Gd generates a spin current upon laser excitation, it should have the opposite sign to the spin current generated by Co.[17,22] Therefore, one could expect that when a Gd layer is added, the total spin current (and THz signal) should either be reduced or change sign (if Gd becomes the dominant contributor). However, no such reduction or sign change is observed in Fig. 1(b), quite the opposite, the signal increases. There are a few possible mechanisms that could explain this increase (Fig. 1(d)): First, the Co generated spin current could be absorbed within the Gd layer, leading to a larger asymmetry between the spin currents entering each Ta layer, thus reducing the destructive interference effect. Additionally, if spin currents from the Gd demagnetization are present, these could result in asymmetric THz due to absorption of Gd spins in the Co layer. This THz could interfere constructively with the ones generated by the Co demagnetization. Finally, Gd could act not only as a spin sink,[23] but also as a spin-to-charge converter.[24] Indeed, according to the literature,[25,26] Gd has a positive spin Hall angle which is opposite to Ta, which would also result in an increase in the THz signal.

Next, we altered the buffer and capping Ta layers to change the sign and amplitude of the top and bottom spin-to-charge converters without changing the spin currents. We checked the signal polarities by flipping the samples as shown in the following Fig. 1 and found always traces

with opposite sign. For the sake of clarity we only show the THz waveforms generated by top (-t) excitation in the figure below. Figure 2(a) shows the THz waveforms generated from sub/Ta(3)/Cu(4)/Co(2)/Gd(1)/Cu(4)/Ta(5), sub/Ta(3)/Cu(4)/Co(2)/Gd(1)/Cu(4)/Pt(3) and sub/Pt(3)/Cu(4)/Co(2)/Gd(1)/Cu(4)/Ta(5) samples (see Fig. S1 in supplemental material for full curves). The thin Cu layers were used to keep the interfaces with the magnetic layers constant as we changed the capping and buffer layers, and inserted MgO, even if these thin Cu layers result in a significant decrease in the THz emission as has been well documented.[27,28] Ta and Pt have opposite spin Hall angles, so when the top Ta(5) is replaced by Pt(3) in the sub/Ta/Cu/Co/Gd/Cu/Pt sample, the charge currents in the Ta(3) and Pt(3) layers flow in the same direction. Figure 2(a) shows an increase in the THz signal for sub/Ta/Cu/Co/Gd/Cu/Pt. The lack of sign change when substituting the top Ta(5) layer for Pt (which has a larger and opposite spin Hall angle) also indicates that the charge current on the Ta(3) side is dominating the THz emission (see Figs. 2(a) and 2(b)). Therefore, by replacing this dominating Ta(3) layer by a Pt layer in the sub/Pt/Cu/Co/Gd/Cu/Ta sample, we logically observe an inverted THz signal with increased amplitude (see Figs. 2(a) and 2(b)). Finally, we notice that the laser absorption in the Gd layer in the sub/Pt/Cu/Co/Gd/Cu/Ta should be larger for the top (-t) excitation rather than the substrate (-s) one (see Fig. S2 in the supplemental material). However, as shown in Fig. S1, the emission is weaker in the top excitation case. This indicates that Gd heating and the spin currents it generates do not significantly contribute to the THz signal.

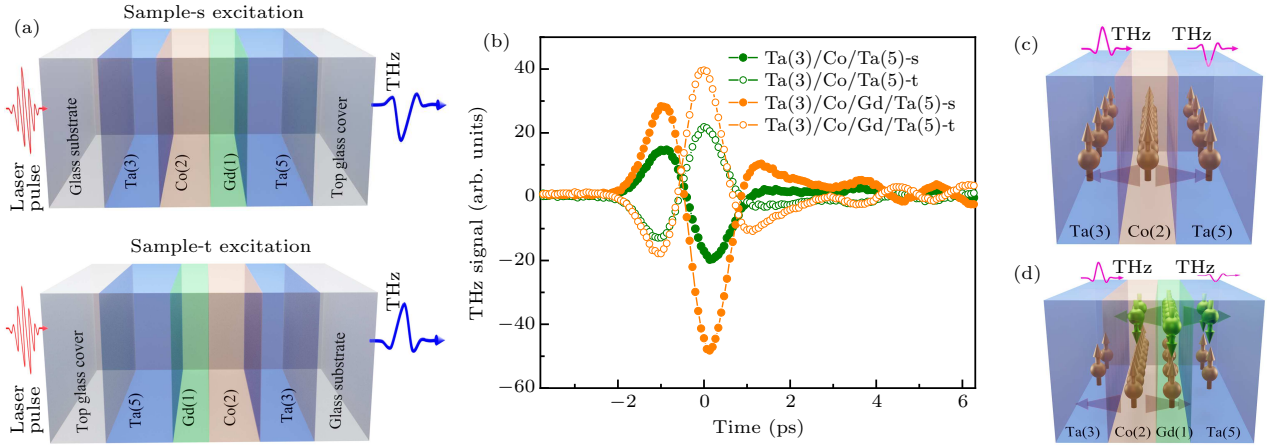


Fig. 1. (a) Schematic representation of the polarity of the generated THz waves. The femtosecond laser is incident on the substrate side: sample-s excitation or on the top side: sample-t excitation. (b) THz waveforms from sub/Ta(3 nm)/Co(2 nm)/Ta(5 nm) and sub/Ta(3 nm)/Co(2 nm)/Gd(1 nm)/Ta(5 nm). (c) Schematic illustration of THz emission from sub/Ta(3 nm)/Co(2 nm)/Ta(5 nm). The spin currents generated from Co layer transport into both top and bottom Ta layers (purple arrows) lead to THz waves with opposite phase. (d) Schematic illustration of THz emission from sub/Ta(3 nm)/Co(2 nm)/Gd(1 nm)/Ta(5 nm). The spin current generated from Gd has the opposite sign to that generated by Co, and flows (green arrows) to both the top and bottom Ta layers. The absorption of Co spins by the Gd layer, or *vice versa*, results in asymmetric THz.

We then attempted to block some of the top and bottom spin currents by adding an MgO insulating layer in the stack. Figure 2(c) shows the THz waveforms generated from sub/Ta(3)/Cu(4)/Co(2)/Gd(1)/Cu(2)/MgO(5)/Cu(2)/Ta(5) and sub/Ta(3)/Cu(2)/MgO(5)/Cu(2)/Co(2)/Gd(1)/Cu(4)/Ta(5) samples (see Fig. S3 in supplemental material for full curves). The waveform shapes differ significantly between these two samples (three versus two maxima or minima). When the MgO layer blocks the top spin current travelling towards the Ta(5) cap, the overall shape of the THz waveform remains similar to those in Fig. 2(a). Once again, this result confirms that it is the spin current travelling down into the buffer Ta(3) layer that dominates the THz generation (see Fig. 2(d)). However, introducing an MgO layer beneath the magnetic stack leads to a significant alteration in the THz waveform. This bottom MgO layer blocks the spin current travelling down into the buffer Ta(3) layer. Therefore, the spin current travelling into the Ta(5) cap layer dominates the THz generation. Two scenarios could explain the change of THz waveform. In one scenario, Gd generates THz spin currents. The injection of Gd spins, which are opposite to Co spins, into the Ta(5) layer causes competition between opposite THz polarities, resulting in the different shape. The other possibility is that Gd acts as a spin-to-charge converter. In this case, the spin Hall currents in the Gd and Ta(5) layers flow in opposite directions, and this competition results in the different shape (see Fig. 2(d)).

Finally, we discuss and test the timescales and frequency responses of the expected spin currents. Upon laser excitation in single elemental magnets, the demagnetization of a Co system is fast, within 100 fs,[29] whereas Gd is typically very slow, taking tens of ps,[17] due to its low Curie temperature (T_c) and the critical slowdown.[30] However, in alloys, a much faster demagnetization time[20] as well as spin currents[22] have been observed, which can be attributed to the exchange coupling with Co increasing the T_c of Gd. Nevertheless, in Co/Gd multilayers, the overall T_c of the Gd layer as a function of thickness is less clear, and much slower responses from the Gd system have been identified.[17] There-

fore, we speculate that, in our bilayer systems, Gd may contribute with a much slower signal appearing at sub-THz frequencies. For this reason, we performed several long scans of the sub/Ta/Co/Gd/Ta and sub/Ta/Co/Ta samples, with the intention of finding the Gd signal by comparing the waveforms of these two samples. Figure 3 shows the THz waveforms generated from sub/Ta/Co/Ta and sub/Ta/Co/Gd/Ta samples within the long scan. For ease of observation, we divided the horizontal coordinate Time into two intervals. By comparing the two waveforms, no signals unique to the sub/Ta/Co/Gd/Ta sample were observed. According to these experimental results, we cannot probe any slower spin current from the Gd using THz time-domain spectroscopy. Lichtenberg *et al.*[17] measured THz standing spin-waves as well as GHz homogeneous precessional modes of Co/Gd bilayers and probed both the high- and low- frequency components of the spin currents. The low-frequency homogeneous mode suggests a significant contribution of Gd to the spin current but measurements on the THz frequency spin waves reveal the inability of the Gd-generated spin currents to excite dynamics at the subpicosecond timescale. Our results are therefore fully compatible with Lichtenberg's observation.

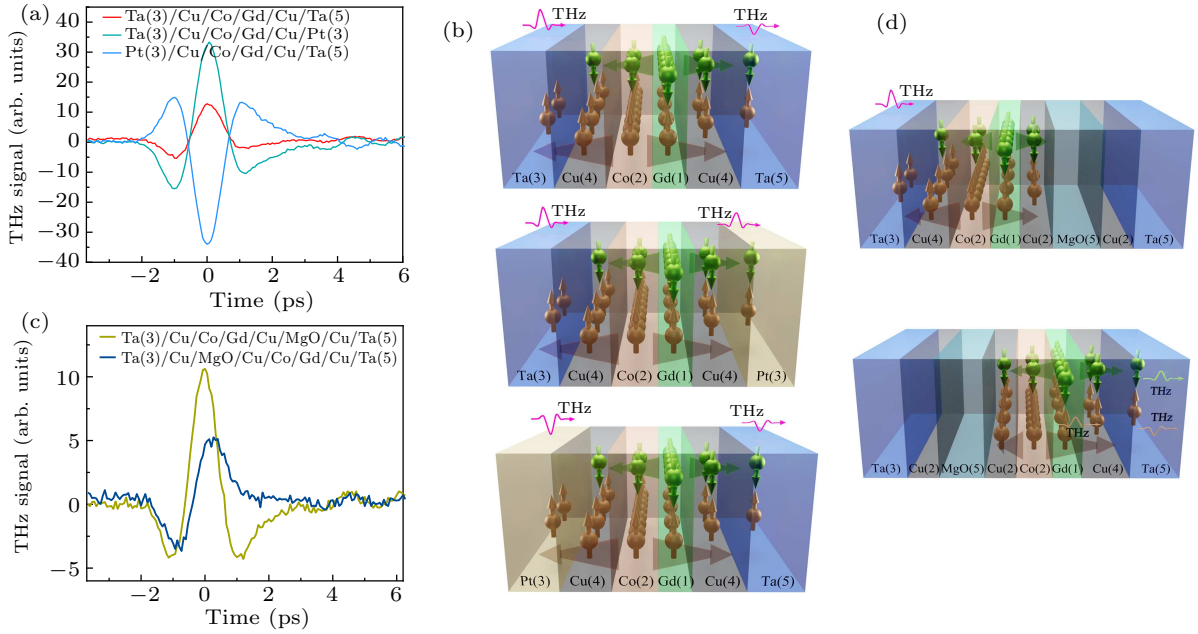


Fig. 2. (a) The THz waveforms and (b) the schematic illustration of the THz emission from sub/Ta(3)/Cu(4)/Co(2)/Gd(1)/Cu(4)/Ta(5), sub/Ta(3)/Cu(4)/Co(2)/Gd(1)/Cu(4)/Pt(3) and sub/Pt(3)/Cu(4)/Co(2)/Gd(1)/Cu(4)/Ta(5). The charge currents in the Ta and Pt layers flow in the same direction and radiate the same phase of THz. (c) THz waveforms and (d) schematic illustration of THz emission from sub/Ta(3)/Cu(4)/Co(2)/Gd(1)/Cu(2)/MgO(5)/Cu(2)/Ta(5) and sub/Ta(3)/Cu(2)/MgO(5)/Cu(2)/Co(2)/Gd(1)/Cu(4)/Ta(5). When the MgO layer blocks the top spin current travelling towards the Ta(5) cap, the spin current travelling down into the buffer Ta(3) layer dominates the THz generation. With the bottom MgO layer, the THz emission is governed by the top Ta(5) layer. The injection of Gd spins (which are opposite to Co spins) into the Ta(5) layer causes competition of opposite THz polarity (green THz line and orange THz line in the Ta(5) layer). Gd also acts as a spin-to-charge converter (orange THz line in the Gd layer). The numbers in brackets indicate the thickness in unit nm.

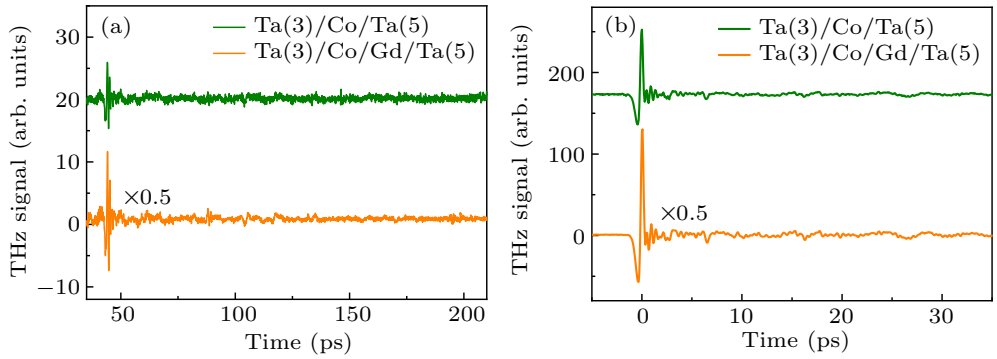


Fig. 3. THz waveforms generated from sub/Ta(3 nm)/Co(2 nm)/Ta(5 nm) and sub/Ta(3 nm)/Co(2 nm)/Gd(1 nm)/Ta(5 nm) samples within the long scan.

4. Conclusion

In summary, we have shown that the spin current from Gd cannot be probed by THz time-domain spectroscopy by performing THz emission experiments on some Co/Gd samples. We attribute this limitation to the fact that Gd demagnetization may be too slow and the spin current generated from Gd is unable to produce THz radiation. This means that even though a Co/Gd bilayer resulted in higher emission than the bare Co

sample, such enhancement is not the results of additional Gd-induced spin currents. Selective probing of the different demagnetizations and/or spin currents of the different elements in ferrimagnetic systems remains an important challenge.

Acknowledgements

Project supported by the National Key Research and Development Program of China (Grant No. 2023YFF0719200), the National Natural Science Foundation of China (Grant No. 62105011), and the French National Research Agency ANR through the UFO project (Grant No. ANR-20-CE09-0013), the SLAM project (Grant No. ANR-23-CE30-0047), the MAT-PULSE-Lorraine Université d'Excellence project (Grant No. ANR-15-IDEX-04-LUE), and through the France 2030 Government Grants PEPR Electronic EMCOM (Grant No. ANR-22-PEEL-0009).

References

[1] Beaurepaire E, Merle J C, Daunois A and Bigot J Y 1996 *Phys. Rev. Lett.* **76** 4250
[2] Stanciu C D, Hansteen F, Kimel A V, Kirilyuk A, Tsukamoto A, Itoh A and Rasing T 2007 *Phys. Rev. Lett.* **99** 047601
[3] Liu X, Xu Z, Gao R, Hu H, Chen Z, Wang Z, Du J, Zhou S and Lai T 2008 *Appl. Phys. Lett.* **92** 232501
[4] Lalieu M L M, Peeters M J G, Haenen S R R, Lavrijsen R and Koopmans B 2017 *Phys. Rev. B* **96** 220411
[5] Malinowski G, Dalla Longa F, Rietjens J H H, Paluskar P V, Huijink R, Swagten H J M and Koopmans B 2008 *Nat. Phys.* **4** 855
[6] Battiato M, Carva K and Oppeneer P M 2010 *Phys. Rev. Lett.* **105** 027203
[7] Choi G M, Min B C, Lee K J and Cahill D G 2014 *Nat. Commun.* **5** 4334
[8] Shokeen V, Sanchez Piaia M, Bigot J Y, Muller T, Elliott P, Dewhurst J K, Sharma S and Gross E K U 2017 *Phys. Rev. Lett.* **119** 107203
[9] Iihama S, Xu Y, Deb M, Malinowski G, Hehn M, Gorchon J, Fullerton E E and Mangin S 2018 *Adv. Mater.* **30** e1804004
[10] Hennecke M, Radu I, Abrudan R, Kachel T, Holldack K, Mitzner R, Tsukamoto A and Eisebitt S 2019 *Phys. Rev. Lett.* **122** 157202
[11] Rouzegar R, Brandt L, Nádvorník L, Reiss D A, Chekhov A L, Gueckstock O, In C, Wolf M, Seifert T S, Brouwer P W, Woltersdorf G and Kampfrath T 2022 *Phys. Rev. B* **106** 144427
[12] Remy Q, Hohlfeld J, Verges M, Le Guen Y, Gorchon J, Malinowski G, Mangin S and Hehn M 2023 *Nat. Commun.* **14** 445
[13] van Hees Y L W, van de Meugheuvel P, Koopmans B and Lavrijsen R 2020 *Nat. Commun.* **11** 3835
[14] Remy Q, Igarashi J, Iihama S, Malinowski G, Hehn M, Gorchon J, Hohlfeld J, Fukami S, Ohno H and Mangin S 2020 *Adv. Sci.* **7** 2001996
[15] Huisman T J, Ciccarelli C, Tsukamoto A, Mikhaylovskiy R V, Rasing T and Kimel A V 2017 *Appl. Phys. Lett.* **110** 072402
[16] Huisman T J, Mikhaylovskiy R V, Tsukamoto A, Rasing T and Kimel A V 2015 *Phys. Rev. B* **92** 104419
[17] Lichtenberg T, van Hees Y L W, Beens M, Levels C J, Lavrijsen R, Duine R A and Koopmans B 2022 *Phys. Rev. B* **106** 094436
[18] Miao B F, Huang S Y, Qu D and Chien C L 2013 *Phys. Rev. Lett.* **111** 066602
[19] Chen X, Wang H, Liu H, Wang C, Wei G, Fang C, Wang H, Geng C, Liu S, Li P, Yu H, Zhao W, Miao J, Li Y, Wang L, Nie T, Zhao J and Wu X 2022 *Adv. Mater.* **34** e2106172
[20] Radu I, Vahaplar K, Stamm C, Kachel T, Pontius N, Durr H A, Ostler T A, Barker J, Evans R F, Chantrell R W, Tsukamoto A, Itoh A, Kirilyuk A, Rasing T and Kimel A V 2011 *Nature* **472** 205
[21] Haskel D, Srajer G, Lang J C, Pollmann J, Nelson C S, Jiang J S and Bader S D 2001 *Phys. Rev. Lett.* **87** 207201
[22] Choi G M and Min B C 2018 *Phys. Rev. B* **97** 014410
[23] Bansal R, Chowdhury N and Muduli P K 2018 *Appl. Phys. Lett.* **112** 262403
[24] Wu Y, Elyasi M, Qiu X, Chen M, Liu Y, Ke L and Yang H 2016 *Adv. Mater.* **29** 1603031
[25] Cui B, Zhu Z, Wu C, Guo X, Nie Z, Wu H, Guo T, Chen P, Zheng D, Yu T, Xi L, Zeng Z, Liang S, Zhang G, Yu G and Wang K L 2022 *Nanomaterials (Basel)* **12** 1887
[26] Reynolds N, Jadaun P, Heron J T, Jermain C L, Gibbons J, Collette R, Buhrman R A, Schlom D G and Ralph D C 2017 *Phys. Rev. B* **95** 064412
[27] Gorchon J, Mangin S, Hehn M and Malinowski G 2022 *Appl. Phys. Lett.* **121** 012402
[28] Seifert T S, Tran N M, Gueckstock O, Rouzegar S M, Nadvornik L, Jaiswal S, Jakob G, Temnov V V, Münzenberg M, Wolf M, Kläui M and Kampfrath T 2018 *J. Phys. D: Appl. Phys.* **51** 364003
[29] Hennes M, Lambert G, Chardonnet V, Delaunay R, Chiuzbăian G S, Jal E and Vodungbo B 2022 *Appl. Phys. Lett.* **120** 072408
[30] Koopmans B, Malinowski G, Dalla Longa F, Steiauf D, Fahnle M, Roth T, Cinchetti M and Aeschlimann M 2010 *Nat. Mater.* **9** 259